

Reconciling π phase shift in Josephson junction experiments with even-parity superconductivity in Sr_2RuO_4

Austin W. Lindquist¹ and Hae-Young Kee^{1,2,*}

¹*Department of Physics and Center for Quantum Materials, University of Toronto, 60 St. George St., Toronto, Ontario, M5S 1A7, Canada*
²*Canadian Institute for Advanced Research, Toronto, Ontario, M5G 1Z8, Canada*

The superconducting state of Sr_2RuO_4 was once thought to be a leading candidate for p -wave superconductivity. A constant Knight shift below the transition temperature provided evidence for spin-triplet pairing, and a π phase shift observed in Josephson junction tunneling experiments suggested odd-parity pairing, both of which are described by p -wave states. However, with recent experiments observing a significant decrease in the Knight shift below the transition temperature, signifying a spin-singlet state, the odd-parity results are left to be reconciled. In this work, we show that an even-parity pseudospin-singlet state originating from interorbital pairing via spin-orbit coupling can explain what has been assumed to be evidence for an odd-parity state. In the presence of small mirror symmetry breaking, interorbital pairing is uniquely capable of displaying odd-parity characteristics required to explain these experimental results. Further, we discuss how these experiments may be used to differentiate the proposed pairing states of Sr_2RuO_4 .

I. INTRODUCTION

The puzzle of superconductivity in Sr_2RuO_4 (SRO) has been a longstanding problem with many seemingly contradictory experimental results [1–4]. Once a leading candidate for $p+ip$ -wave spin-triplet superconductivity [5, 6], recent experiments show a drop in the Knight shift below the superconducting transition temperature, potentially ruling this state out [7–9]. Other notable experiments suggest a two component order parameter [10–12] which breaks time-reversal symmetry [13–16] and features gap nodes [17–19]. Attempts to explain these results have led to the recent proposals of various multicomponent, even-parity pairing states [20–28].

The proposed even-parity states are capable of explaining many experimental results, however, little progress has been made in explaining the experimental data supporting odd-parity superconductivity [29–32]. Primarily, phase-sensitive Josephson junction experiments observe a π phase shift of the superconducting order parameter under inversion [29]. Previous studies have shown these results to be consistent with odd-parity pairing [33, 34], whereas conventional even-parity spin-singlet states have remained in contradiction with these observations. Conventional even-parity superconductors with inversion symmetry breaking have been shown to display both even- and odd-parity character in non-centrosymmetric superconductors [35, 36], however, this effect would be much smaller in SRO.

In this work, we study even-parity intraband pseudospin-singlet superconductivity, evolved from interorbital spin-triplet pairing via spin-orbit coupling (SOC) in the presence of small mirror symmetry breaking hoppings as a route to reconcile these remaining contradictions. The mirror symmetry breaking hopping term we introduce occurs near surfaces, interfaces, or strain as sketched in the experimental setup shown in Fig. 1a in Sec. II. We then explain the setup of the Josephson junction calculations in Sec. III and show the current-phase relations for conventional even- and

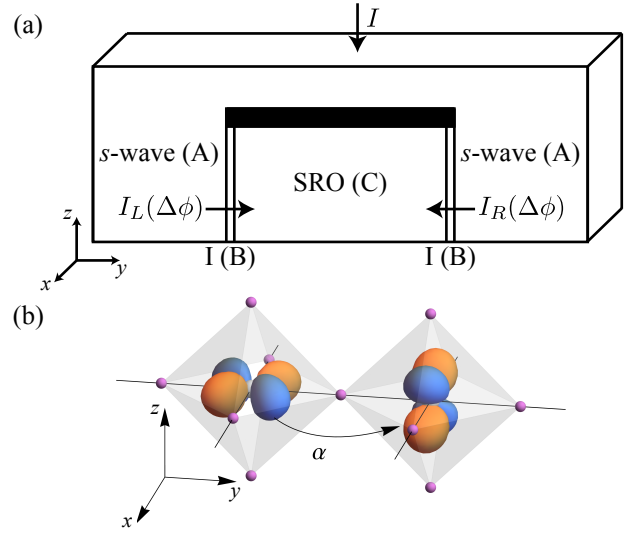


Figure 1. (a) Schematic of the Josephson junction setup showing the s -wave superconductor, insulator (I), and SRO regions, denoted A, B, and C in the main-text equations, labeled here in parentheses. In experiment SRO and the s -wave superconductor are separated in the z -direction by SiO, and no tunneling occurs at this interface, signified by the filled black region here. (b) One example of interorbital hopping which is only allowed where mirror symmetry is broken. When a z -mirror plane exists, the orbital overlap is 0, but when broken, the overlap is finite.

odd-parity pairing states. Finally, in Sec. IV we present interorbital pairing and show that signatures of pairing states which feature gap nodes in the tunneling direction may match those expected of an odd-parity state. This behavior is made possible by the multiorbital nature of SRO and the intraband pseudospin-singlet pairing evolved from interorbital spin-triplet pairing.

* hy.ke@utoronto.ca

II. MICROSCOPIC HAMILTONIAN

The Josephson junction consists of a conventional single band s -wave superconducting region, a normal insulator region, and the superconducting SRO region. A schematic of the regions is shown in Fig. 1(a), and they are denoted A , B , and C , respectively, in the equations below. Within regions A and B we use the single band kinetic Hamiltonian, written here for region A ,

$$H_A = \sum_{\mathbf{k}, i_y, \delta_y, \sigma} \xi_A(\mathbf{k}, \delta_y) c_{A, \mathbf{k}, i_y, \sigma}^\dagger c_{A, \mathbf{k}, i_y + \delta_y, \sigma} \quad (1)$$

where $\xi_A(\mathbf{k}, \delta_y)$ is the electron dispersion in region A between slabs at positions i_y and $i_y + \delta_y$, and $c_{A, \mathbf{k}, i_y, \sigma}^\dagger$ creates an electron in slab i_y of region A with momentum $\mathbf{k} = (k_x, k_z)$ and spin σ . The form of all dispersion terms as well as the values of the hopping parameters are given in Appendix A. The superconductivity in region A is described by,

$$H_A^{\text{SC}} = \sum_{\mathbf{k}, i_y} e^{i\phi_A} \Delta_A c_{A, \mathbf{k}, i_y, \uparrow}^\dagger c_{A, -\mathbf{k}, i_y, \downarrow}^\dagger + \text{h.c.}, \quad (2)$$

where Δ_A is the s -wave order parameter, and ϕ_A is the superconducting phase. Hopping between regions A and B is taken to have the same parameters as hopping within either of the regions.

The normal state Hamiltonian of region C is,

$$H_C = \sum_{\mathbf{k}, i_y, a, \sigma} \xi_C^a(\mathbf{k}, \delta_y) c_{C, \mathbf{k}, i_y, \sigma}^\dagger c_{C, \mathbf{k}, i_y + \delta_y, \sigma}^a + \sum_{\mathbf{k}, i_y, a \neq b, \sigma} \xi_C^{ab}(\mathbf{k}, \delta_y) c_{C, \mathbf{k}, i_y, \sigma}^\dagger c_{C, \mathbf{k}, i_y + \delta_y, \sigma}^b + \text{h.c.} + H_{\text{SOC}}, \quad (3)$$

which includes intraorbital and interorbital dispersions, $\xi_C^a(\mathbf{k}, \delta_y)$ and $\xi_C^{ab}(\mathbf{k}, \delta_y)$, respectively, where a and b are the orbital indices representing the yz , xz , and xy orbitals, as well as SOC terms. Finally, the Hamiltonian describing hopping between regions B and C , where the interface occurs between $i_y = 1$ and 2 , has the form,

$$H_{\text{int}} = \sum_{\mathbf{k}, a, \sigma} \xi_{\text{int}}^a(\mathbf{k}) c_{C, \mathbf{k}, 2, \sigma}^\dagger c_{B, \mathbf{k}, 1, \sigma} + \text{h.c.}, \quad (4)$$

which features orbital dependence in the SRO region, as denoted by $\xi_{\text{int}}^a(\mathbf{k})$.

We also consider the effects of mirror symmetry breaking in the z -direction (out of plane direction). This effect is largest near the surface normal to the z -direction, but imperfections of the interface leading to a broken mirror plane in the z -direction have previously been proposed to occur [37], where it was shown that the experimental results may be explained by a $d_{xz} + id_{yz}$ -wave state if the tunneling directions tilt out of the xy plane. Additionally, the growth of $\text{Au}_{0.5}\text{In}_{0.5}$ directly onto SRO to create the junction may cause strain in SRO. Any deformations of the lattice that this leads to may further contribute to broken mirror symmetry throughout the sample. Dislocations may also contribute to this mirror symmetry breaking, and have been found to occur near interfaces [38]. The lack of

mirror symmetry in the z -direction means that hopping between the xy and $xz(yz)$ orbitals is allowed to be finite in the $y(x)$ direction. An example of such hopping is shown in Fig. 1(b) for the xy to xz interorbital hopping. These hoppings have the form:

$$h_{\mathbf{k}}^{ISB} = -\alpha [2i \sin k_x (c_{\mathbf{k}, i_y, \sigma}^{yz\dagger} c_{\mathbf{k}, i_y, \sigma}^{xy} - c_{\mathbf{k}, i_y, \sigma}^{xy\dagger} c_{\mathbf{k}, i_y, \sigma}^{yz}) - (c_{C, \mathbf{k}, i_y, \sigma}^{xz\dagger} c_{C, \mathbf{k}, i_y + 1, \sigma}^{xy} - c_{C, \mathbf{k}, i_y, \sigma}^{xy\dagger} c_{C, \mathbf{k}, i_y + 1, \sigma}^{xz} + \text{h.c.})], \quad (5)$$

where α represents the hopping integral, which depends on the strength of the mirror symmetry breaking, and the use of $\delta_y = 1$ here represents nearest-neighbor hopping between slabs.

In the next section, we describe the setup for the Josephson tunneling calculations and apply it with conventional s - and p -wave superconducting states in the SRO region. Then, we consider interorbital superconductivity and show how the current-phase relation (CPR) is affected by the mirror symmetry breaking terms introduced here, showing that they may behave like the conventional s -wave state, or potentially more like the p -wave state, depending on the nodal structure as well as the strength of the mirror symmetry breaking.

III. JOSEPHSON CALCULATIONS

To calculate the Josephson CPR, we use the lattice Green's function method presented in Ref. 34, which considers only p -wave pairing to explain experimental results. Semi-infinite Green's functions are obtained for the s -wave and SRO regions using the recursive Green's function approach [39]. A single layer of the normal insulator is added on the surfaces of both of these regions by the Dyson equations,

$$\hat{G}_0^B(\mathbf{k}, i\omega_l) = (i\omega_l - \hat{u}_0(\mathbf{k}) - \hat{t}_{0,-1} \hat{G}_{-1}^A(\mathbf{k}, i\omega_l) \hat{t}_{-1,0})^{-1}, \quad (6)$$

$$\hat{G}_1^B(\mathbf{k}, i\omega_l) = (i\omega_l - \hat{u}_1(\mathbf{k}) - \hat{t}_{1,2} \hat{G}_2^C(\mathbf{k}, i\omega_l) \hat{t}_{2,1})^{-1}, \quad (7)$$

where the interface is in the xz plane. Here, $\hat{G}_n^m(\mathbf{k}, i\omega_l)$ is the Green's function of layer n in region m , $\hat{u}_n(\mathbf{k})$ is the part of the Hamiltonian of layer n , and $\hat{t}_{n,n+1}$ is the part of the Hamiltonian featuring hopping the the y -direction, representing hopping between layers n and $n+1$. The left and right systems are combined using the two equations,

$$\hat{G}_{00}(\mathbf{k}, i\omega_l) = \{[\hat{G}_0^B(\mathbf{k}, i\omega_l)]^{-1} - \hat{t}_{01} \hat{G}_1^B(\mathbf{k}, i\omega_l) \hat{t}_{10}\}^{-1}, \quad (8)$$

$$\hat{G}_{11}(\mathbf{k}, i\omega_l) = \{[\hat{G}_1^B(\mathbf{k}, i\omega_l)]^{-1} - \hat{t}_{10} \hat{G}_0^B(\mathbf{k}, i\omega_l) \hat{t}_{01}\}^{-1}. \quad (9)$$

These are then used to obtain the nonlocal Green's functions

$$\hat{G}_{01}(\mathbf{k}, i\omega_l) = \hat{G}_0^B(\mathbf{k}, i\omega_l) \hat{t}_{01} \hat{G}_{11}(\mathbf{k}, i\omega_l), \quad (10)$$

$$\hat{G}_{10}(\mathbf{k}, i\omega_l) = \hat{G}_1^B(\mathbf{k}, i\omega_l) \hat{t}_{10} \hat{G}_{00}(\mathbf{k}, i\omega_l). \quad (11)$$

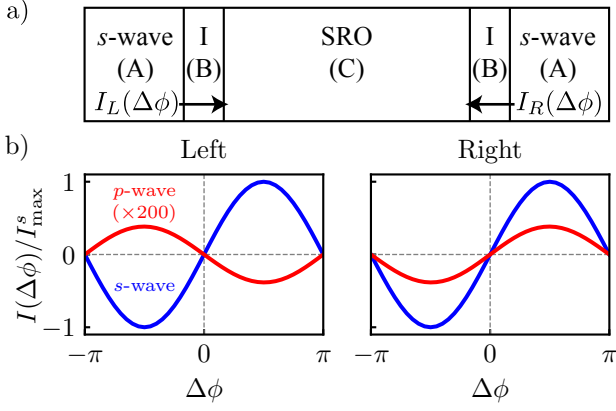


Figure 2. (a) Schematic of the setup for CPR calculations, showing the left and right interfaces between the s -wave SC and SRO. (b) Current-phase relations for both s -wave SC/I/SRO interfaces with the SRO region modelled using an intraorbital s - and p -wave pairing state.

From this, the CPR, $I(\Delta\phi)$, is obtained,

$$I(\Delta\phi) = \frac{iet}{\hbar} \int_{-\pi}^{\pi} \text{Tr}' \frac{1}{\beta} \sum_l [\hat{G}_{01}(\mathbf{k}, i\omega_l, \Delta\phi) - \hat{G}_{10}(\mathbf{k}, i\omega_l, \Delta\phi)] d\mathbf{k}, \quad (12)$$

where Tr' represents a trace over only the electron space, $\beta = \frac{1}{k_B T}$, t is the nearest-neighbor hopping integral in the normal region, and $\Delta\phi = \phi_A - \phi_C$ represents the phase difference in the superconducting phase of the s -wave and SRO regions.

To understand the CPRs of the Josephson π junction, we first review conventional superconducting states. First, we use an intraorbital s -wave state in the SRO region,

$$H_{C,s}^{\text{SC}} = \sum_{\mathbf{k}, i_y, a} e^{i\phi_C} \Delta_C^a c_{C,\mathbf{k}, i_y, \uparrow}^a c_{C, -\mathbf{k}, i_y, \downarrow}^{a\dagger} + \text{h.c.}, \quad (13)$$

where the order parameter, Δ_C^a , exists within all three orbitals. The explicitly written superconducting phase, ϕ_C , is kept the same between all three orbitals, and calculations were performed with $\Delta_C^{yz} = \Delta_C^{xz} = -\Delta_C^{xy}$, similar to intraorbital s -wave contributions found in Ref. 40. Fig. 2(b) shows the CPR at the left and right interfaces of the π junction for the s -wave pairing state in blue. This shows no phase shift between the two interfaces, as expected for an even-parity pairing state.

Next, we use an intraorbital $p_x + ip_y$ -wave pairing state,

$$H_{C,p}^{\text{SC}} = \sum_{\mathbf{k}, i_y, a} e^{i\phi_C} d_z^a (2 \sin k_x c_{C,\mathbf{k}, i_y, \uparrow}^a c_{C, -\mathbf{k}, i_y, \downarrow}^{a\dagger} + c_{C,\mathbf{k}, i_y, \uparrow}^a c_{C, -\mathbf{k}, i_y, \downarrow}^{a\dagger} - c_{C,\mathbf{k}, i_y, \uparrow}^a c_{C, -\mathbf{k}, i_y, \downarrow}^{a\dagger}) + \text{h.c.} \quad (14)$$

Again, the phase is kept the same between all three orbitals, and the same sign convention is used as in the s -wave pairing state. Fig. 2(b) shows the CPR at the left and right interfaces for the p -wave pairing state in red. Now, the π phase shift is observed between the interfaces, characteristic of the odd-parity state.

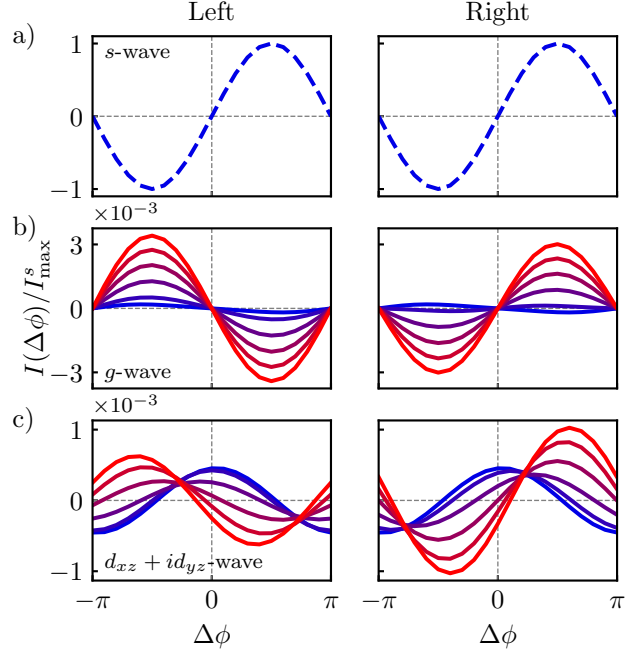


Figure 3. Current-phase relations for an interorbital SC/I/ s -wave interface with a varying mirror symmetry breaking hopping, increasing linearly from 0 to 0.005 in units of $2t = 1$ between the blue and red curves. The left column represents the left interface, and the right represents the right interface. The SRO region is considered here with *interorbital* (a) s - (b) $g_{xy(x^2-y^2)}$ - and (c) $d_{xz} + id_{yz}$ -wave pairing. Only the $\alpha = 0$ curve is shown with the dashed line in (a) as no significant change is observed in the presence of α . The $d_{x^2-y^2}$ - and d_{xy} -wave CPRs (not shown) are qualitatively similar to the s - and $g_{xy(x^2-y^2)}$ -wave curves, respectively.

These two results show a clear distinction between even- and odd-parity pairing. Since the current measured through the entire junction in experiment depends on the addition of these two curves, the odd-parity phase difference corresponds to a minimum current through the junction, as measured in Ref. 29, whereas the even-parity state would correspond to a maximum. While this allows for straightforward differentiation between intraorbital pairing states, in the next section we consider how this changes when interorbital pairing is instead considered, in the presence of broken mirror symmetry.

IV. INTERORBITAL SUPERCONDUCTIVITY

Equipped with the techniques, we now perform the Josephson calculations in multiorbital superconductors. In multiorbital systems, the orbital degree of freedom allows for additional types of pairing which satisfy the antisymmetric fermion wavefunction requirement. In addition to even-parity spin-singlet and odd-parity spin-triplet pairings, even-parity spin-triplet and odd-parity spin-singlet pairings are possible when the wavefunction is antisymmetric with respect to the orbital index. The possibility of interorbital pairing occurring in SRO has been considered in previous studies [40–51], and, importantly, has re-

cently been discussed as a microscopic route to the proposed $s + id_{xy}$ -wave [24], $d_{x^2-y^2} + ig_{xy(x^2-y^2)}$ -wave [25, 28], and $d_{xz} + id_{yz}$ -wave pairing states [21].

The general form of the interorbital superconducting state is written,

$$\hat{\Delta}_{a/b}^{l\dagger} = \frac{1}{4N} \sum_{\mathbf{k}, i_y} [i\hat{\sigma}^y \hat{\sigma}^l]_{\sigma\sigma'} (c_{\mathbf{k}, i_y, \sigma}^{a\dagger} c_{-\mathbf{k}, i_y, \sigma'}^{b\dagger} - c_{\mathbf{k}, i_y, \sigma}^{b\dagger} c_{-\mathbf{k}, i_y, \sigma'}^{a\dagger}). \quad (15)$$

Here, the interorbital pairing is a constant in k -space, i.e., s -wave. However, momentum dependence may be revealed after transforming into the band basis due to momentum-dependent SOC or a combination of dispersion terms and SOC [24, 25].

To understand the momentum dependence of the intraband gap that arises in the presence of broken mirror symmetry, let us first consider a bulk two orbital model which features SOC and a mirror symmetry breaking hopping term. We use the basis $\Psi_{\mathbf{k}}^{\dagger} = (\psi_{\mathbf{k}}^{\dagger}, \mathcal{T}\psi_{\mathbf{k}}^T \mathcal{T}^{-1})$ where \mathcal{T} represents time-reversal, and $\psi_{\mathbf{k}}^{\dagger} = (c_{\mathbf{k}, \uparrow}^{xz\dagger}, c_{\mathbf{k}, \downarrow}^{xz\dagger}, c_{\mathbf{k}, \uparrow}^{xy\dagger}, c_{\mathbf{k}, \downarrow}^{xy\dagger})$. The kinetic and SOC parts of the Hamiltonian are,

$$H_{\mathbf{k}} = \frac{1}{2}\xi^+(\mathbf{k})\rho_3\tau_0\sigma_0 + \frac{1}{2}\xi^-(\mathbf{k})\rho_3\tau_3\sigma_0 + \lambda(\mathbf{k})\rho_3\tau_2\sigma_3 + t(\mathbf{k})\rho_3\tau_1\sigma_0 + \alpha(\mathbf{k})\rho_3\tau_2\sigma_0, \quad (16)$$

where ρ , τ , and σ are Pauli matrices representing the particle-hole, orbital, and spin bases, respectively. The orbital dispersions are $\xi^{\pm}(\mathbf{k}) = \xi^{xz}(\mathbf{k}) \pm \xi^{xy}(\mathbf{k})$, the SOC is $\lambda(\mathbf{k})$, the orbital hybridization is $t(\mathbf{k})$, and mirror symmetry breaking hopping $\alpha(\mathbf{k})$. The precise momentum dependence of each of these terms is left unspecified for this analysis, but all are given in Appendix A for the numerical calculations performed below. Importantly, the mirror symmetry breaking hopping is an odd function in \mathbf{k} , $\alpha(-\mathbf{k}) = -\alpha(\mathbf{k})$, while all other terms are even functions of the form $f(-\mathbf{k}) = f(\mathbf{k})$.

The interorbital-singlet spin-triplet pairing with a d -vector in the z -direction is written as $H_{\text{SC}} = \Delta_z \rho_1 \tau_2 \sigma_3$. Transforming H_{SC} to the band basis, i.e., the basis in which $H_{\mathbf{k}}$ is diagonal, the intraband pseudospin-singlet and pseudospin-triplet pairing can both be identified,

$$H_{\text{SC}} = \Delta^S(\mathbf{k})(\hat{\Delta}_{\mathbf{k},0}^{\alpha} - \hat{\Delta}_{\mathbf{k},0}^{\beta}) + \Delta^T(\mathbf{k})(\hat{\Delta}_{\mathbf{k},z}^{\alpha} - \hat{\Delta}_{\mathbf{k},z}^{\beta}), \quad (17)$$

where the pairing operators are written $\hat{\Delta}_{0(z)}^{\alpha}(\mathbf{k}) = c_{-\mathbf{k}, \downarrow}^{\alpha} c_{\mathbf{k}, \uparrow}^{\alpha} \mp c_{-\mathbf{k}, \uparrow}^{\alpha} c_{\mathbf{k}, \downarrow}^{\alpha}$. The pseudospin-singlet and -triplet coefficients are given by,

$$\Delta^S(\mathbf{k}) = \frac{-i\Delta_z \lambda(\mathbf{k})}{\sqrt{\xi^-(\mathbf{k})^2 + 4t(\mathbf{k})^2 + 4\lambda(\mathbf{k})^2}} + \dots, \quad (18)$$

and

$$\Delta^T(\mathbf{k}) = \frac{i\Delta_z \alpha(\mathbf{k})}{\sqrt{\xi^-(\mathbf{k})^2 + 4t(\mathbf{k})^2 + 4\lambda(\mathbf{k})^2}} + \dots, \quad (19)$$

where (\dots) represents higher order terms in the Taylor expansions. Further details of these equations are given in Appendix B. Importantly, there exists a pseudospin-singlet gap contribution proportional to $\lambda(\mathbf{k})\Delta_z$, as well as

a pseudospin-triplet contribution proportional to $\alpha(\mathbf{k})\Delta_z$, both of the same order. Note that the momentum dependence of these two gap coefficients are independent, and locations of nodes in the singlet gap do not necessarily correspond to nodes in the triplet gap.

For comparison, this same analysis is applied to an intraorbital SC state of the form,

$$H'_{\text{SC}} = \Delta^+(\mathbf{k})\rho_1\tau_0\sigma_0 + \Delta^-(\mathbf{k})\rho_1\tau_3\sigma_0, \quad (20)$$

where $\Delta^{\pm}(\mathbf{k}) = \frac{1}{2}(\Delta^{xz}(\mathbf{k}) \pm \Delta^{xy}(\mathbf{k}))$ in this two orbital model. Again transforming this into the band basis, the pairing Hamiltonian is rewritten in terms of the intraband contributions,

$$H'_{\text{SC}} = \Delta^{S'_1}(\mathbf{k})(\hat{\Delta}_0^{\alpha} + \hat{\Delta}_0^{\beta}) + \Delta^{S'_2}(\mathbf{k})(\hat{\Delta}_0^{\alpha} - \hat{\Delta}_0^{\beta}) + \Delta^{T'}(\mathbf{k})(\hat{\Delta}_z^{\alpha} - \hat{\Delta}_z^{\beta}). \quad (21)$$

The first singlet coefficient remains unchanged between the bases, $\Delta^{S'_1}(\mathbf{k}) = \Delta^+(\mathbf{k})$. The other singlet coefficient is,

$$\Delta^{S'_2}(\mathbf{k}) = \frac{\Delta^-(\mathbf{k})\xi^-(\mathbf{k})}{\sqrt{\xi^-(\mathbf{k})^2 + 4t(\mathbf{k})^2 + 4\lambda(\mathbf{k})^2}} + \dots, \quad (22)$$

and the triplet coefficient,

$$\Delta^{T'}(\mathbf{k}) = \frac{4\Delta^-(\mathbf{k})\alpha(\mathbf{k})\xi^-(\mathbf{k})\lambda(\mathbf{k})}{[\xi^-(\mathbf{k})^2 + 4t(\mathbf{k})^2 + 4\lambda(\mathbf{k})^2]^{3/2}} + \dots. \quad (23)$$

In this case, the odd-parity contribution is very small since it only shows up at a higher order expansion. Additionally, since the momentum dependence of the gap is encoded in $\Delta^-(\mathbf{k})$, any nodes that appear within the pseudospin-singlet pairing gap must also be nodes in the pseudospin-triplet gap. Therefore, the effect of the mirror symmetry breaking hopping term on an intraorbital pairing state is not expected to be significant for small $\alpha(\mathbf{k})$. The contrast between these two cases is important. For an interorbital SC state, it is possible to induce a non-zero odd-parity gap where the original even-parity gap has a node. However, for an intraorbital SC state, the induced odd-parity gap must have nodes wherever the original even-parity state has nodes.

Based on Eqs. (18) and (19), there are three significant contributions to the CPR at a given interface that we can write qualitatively,

$$I(\phi) \sim c_1(\Delta\lambda(\mathbf{k})) \sin \phi + c_2(\Delta\alpha(\mathbf{k})) \sin 2\phi + c_3(\Delta\alpha(\mathbf{k})) \sin \phi, \quad (24)$$

where c_i are the coefficients of the various contributions. The first, $c_1(\lambda(\mathbf{k})\Delta_z)$, describes Josephson tunneling from the pseudospin-singlet state of SRO to the spin-singlet state of the s -wave superconductor. The contributing gap is even parity and therefore this term does not feature a π phase shift between opposite interfaces. Next, $c_2(\alpha(\mathbf{k})\Delta_z)$ describes the first pseudospin-triplet to spin-singlet tunneling process. Since this is direct pseudospin-triplet to spin-singlet tunneling, this term features a $\sin 2\phi$ dependence. If the intermediate region is insulating, then the $\sin 2\phi$ contribution is small, and in the presence of SOC, there is again a $\sin \phi$ with coefficient $c_3(\alpha(\mathbf{k})\Delta_z)$ term that contributes.

This term is due to the odd-parity gap and therefore features a π phase shift between opposite interfaces.

The overall behaviour depends on the relative size of these coefficients. The largest coefficient is generally $c_1(\lambda(\mathbf{k})\Delta_z)$ since $|\lambda(\mathbf{k})| > |\alpha(\mathbf{k})|$ is expected, but when $\lambda(\mathbf{k})$ features nodes, this is not always true. For the d_{xy} - and $g_{xy(x^2-y^2)}$ -wave states, nodes exist along the x - and y -directions, so an interface in the (010) direction may feature competition between the $\lambda(\mathbf{k})\Delta_z$ gap and the $\alpha(\mathbf{k})\Delta_z$ due to a small $\lambda(\mathbf{k})$. Alternatively, the $d_{xz} + id_{yz}$ -wave state is gapless in the $z = 0$ plane and therefore any tunneling direction perpendicular to the c -axis would feature this competition. In both cases, if the intermediate region is insulating, the $c_2(\alpha(\mathbf{k})\Delta_z)$ contribution is small compared to the $c_3(\alpha(\mathbf{k})\Delta_z)$ allowing for a path to a π phase shift from one of these even-parity states.

To confirm the above analysis works for the 3-orbital model of SRO, calculations were performed on the full 3-orbital system using various superconducting states. Fig. 3(a) shows the CPR for the s -wave state. The addition of the mirror symmetry breaking hopping has no significant effect on the CPR and is omitted in these plots. This is consistent with expectations from the two-orbital analysis above, since the pairing state does not feature nodes along the (010) direction. Fig. 3(b) shows the CPR for the $g_{xy(x^2-y^2)}$ -wave pairing state. The effect of α is much more significant here, and a π phase shift is observed for a large enough value of α . Fig. 3(c) uses the $d_{xz} + id_{yz}$ -wave pairing state where again the effect of α is significant. In this case, the π phase shift does not occur via a simple sign change of the amplitude, but rather as a gradual phase shift due to competition between the contributions from the d_{xz} and d_{yz} components. This shows that a π phase shift is possible even when the pairing is even-parity, as long as nodes are present in the gap structure and a small mirror symmetry breaking hopping is allowed.

The $d_{x^2-y^2}$ - and d_{xy} -wave states are not plotted, but appear very similar to the s - and $g_{xy(x^2-y^2)}$ -wave states, respectively. This is expected based on the nodal structure of each of these states in the (010) direction. Note that if the tunneling direction were instead in the (110) direction then behavior of the $d_{x^2-y^2}$ - and d_{xy} -wave states is expected to switch, with $d_{x^2-y^2}$ instead showing the π phase shift. In such a case, the combined $d_{x^2-y^2} + ig_{xy(x^2-y^2)}$ -wave state is expected to exhibit a π phase shift, similar to the $d_{xz} + id_{yz}$ -wave state.

V. DISCUSSION AND SUMMARY

A full understanding of the superconductivity of SRO has remained elusive despite vast interest, as well as a wide array of experiments performed on the material. Recent results have pushed the community towards potentially adopting an even-parity spin-singlet pairing state, although conventional states of this nature are not able to consistently explain all observations. Interorbital superconductivity has recently been shown to provide a microscopic route to various multi-component pairing states, each capable of explaining a subset of the experimental results [21, 24, 25, 28]. However, Josephson junction experiments

capable of detecting the phase change of a superconducting order parameter between interfaces observe a π phase shift at opposite interfaces of SRO [29]. While this is expected in odd-parity superconductors, these even-parity proposals are left to provide some explanation for this observed behavior.

We've shown that using even-parity interorbital pairing, it is possible to observe a π phase shift between opposite interfaces in these Josephson junction experiments. The s -wave nature of the interorbital pairing in the orbital basis provides a route to finite odd-parity pseudospin-triplet pairing in the band basis, induced by mirror symmetry breaking. Importantly, the induced odd-parity pairing can have a nodal structure independent of the even-parity state since the even- and odd-parity intraband pairings arise from interorbital pairing via different orbital mixing terms. Due to this, Josephson tunneling current in the direction of the even-parity nodes is dominated by the induced odd-parity behavior. This is in contrast to the intraorbital pairing states, where any induced odd-parity character features nodes in the same positions as the original even-parity state, meaning the odd-parity character does not dominate. While the precise tunneling direction within the xy -plane was not determined in experiment [29], the $d_{xz} + id_{yz}$ -wave state is completely gapless within the plane, and therefore these results are expected to hold for any tunneling direction. The other proposals discussed here feature more complex gap structures and therefore would be more sensitive to the tunneling direction. If the multicomponent nature of the SC state is due to an accidental degeneracy, the precise gap structure where tunneling occurs may also be influenced significantly by surface effects.

Experimental determination of the directional dependence of the phase shift would differentiate the proposed pairing states and could provide crucial information for identifying the superconducting pairing of SRO. Specifically, we expect to see no π phase shift when tunneling occurs in a direction far from the in-plane nodes of both gap components. We therefore propose these phase sensitive Josephson junction experiments with a known orientation of the a and b axes as a route to differentiate the various pairing symmetry proposals.

Although only one type of mirror symmetry breaking hopping is considered here, others may contribute to this effect depending on the precise geometry of the surface. Here we focus on the phase shift observed in the Josephson junction experiment [29], however, experiments observing half-quantum vortices also provide evidence for odd-parity spin-triplet pairing, but use samples with a different geometry [31, 32]. These results may also occur due to interorbital pairing with mirror symmetry breaking, but more work is needed to determine if these results are compatible with the pairing states discussed here. Additionally, spatially varying strain in a system with $d_{x^2-y^2}$ - and $g_{xy(x^2-y^2)}$ -wave degeneracy has been proposed as being able to explain these half-quantum vortices [23]. While work still remains to distinguish the various multicomponent even-parity pairing proposals, we believe that directionally resolved phase sensitive measurements can provide an important piece of puzzle of superconductivity in SRO.

ACKNOWLEDGMENTS

We acknowledge support from the Natural Sciences and Engineering Research Council of Canada Discovery Grant 2022-04601. H.Y.K. also acknowledges support from the

Canadian Institute for Advanced Research and the Canada Research Chairs Program. Computations were performed on the Niagara supercomputer at the SciNet HPC Consortium. SciNet is funded by: the Canada Foundation for Innovation under the auspices of Compute Canada; the Government of Ontario; Ontario Research Fund - Research Excellence; and the University of Toronto.

-
- [1] Y. Maeno, H. Hashimoto, K. Yoshida, S. Nishizaki, T. Fujita, J. G. Bednorz, and F. Lichtenberg, Superconductivity in a layered perovskite without copper, *Nature* **372**, 532 (1994).
- [2] A. P. Mackenzie and Y. Maeno, The superconductivity of Sr_2RuO_4 and the physics of spin-triplet pairing, *Rev. Mod. Phys.* **75**, 657 (2003).
- [3] C. Kallin, Chiral p-wave order in Sr_2RuO_4 , *Reports on Progress in Physics* **75**, 042501 (2012).
- [4] A. P. Mackenzie, T. Scaffidi, C. W. Hicks, and Y. Maeno, Even odder after twenty-three years: the superconducting order parameter puzzle of Sr_2RuO_4 , *npj Quantum Materials* **2**, 40 (2017).
- [5] T. M. Rice and M. Sigrist, Sr_2RuO_4 : an electronic analogue of ^3He ?, *Journal of Physics: Condensed Matter* **7**, L643 (1995).
- [6] K. Ishida, H. Mukuda, Y. Kitaoka, K. Asayama, Z. Q. Mao, Y. Mori, and Y. Maeno, Spin-triplet superconductivity in Sr_2RuO_4 identified by ^{17}O Knight shift, *Nature* **396**, 658 (1998).
- [7] A. Pustogow, Y. Luo, A. Chronister, Y.-S. Su, D. A. Sokolov, F. Jerzembeck, A. P. Mackenzie, C. W. Hicks, N. Kikugawa, S. Raghu, and et al., Constraints on the superconducting order parameter in Sr_2RuO_4 from oxygen-17 nuclear magnetic resonance, *Nature* **574**, 72 (2019).
- [8] K. Ishida, M. Manago, K. Kinjo, and Y. Maeno, Reduction of the ^{17}O Knight Shift in the Superconducting State and the Heat-up Effect by NMR Pulses on Sr_2RuO_4 , *Journal of the Physical Society of Japan* **89**, 034712 (2020).
- [9] A. Chronister, A. Pustogow, N. Kikugawa, D. A. Sokolov, F. Jerzembeck, C. W. Hicks, A. P. Mackenzie, E. D. Bauer, and S. E. Brown, Evidence for even parity unconventional superconductivity in Sr_2RuO_4 , *Proceedings of the National Academy of Sciences* **118**, 10.1073/pnas.2025313118 (2021).
- [10] N. Okuda, T. Suzuki, Z. Mao, Y. Maeno, and T. Fujita, Unconventional Strain Dependence of Superconductivity in Spin-Triplet Superconductor Sr_2RuO_4 , *Journal of the Physical Society of Japan* **71**, 1134 (2002).
- [11] S. Benhabib, C. Lupien, I. Paul, L. Berges, M. Dion, M. Nardone, A. Zitouni, Z. Q. Mao, Y. Maeno, A. Georges, L. Taillefer, and C. Proust, Ultrasound evidence for a two-component superconducting order parameter in Sr_2RuO_4 , *Nature Physics* **17**, 194 (2021), 2002.05916.
- [12] S. Ghosh, A. Shekhter, F. Jerzembeck, N. Kikugawa, D. A. Sokolov, M. Brando, A. P. Mackenzie, C. W. Hicks, and B. J. Ramshaw, Thermodynamic Evidence for a Two-Component Superconducting Order Parameter in Sr_2RuO_4 , *Nature Physics* **17**, 199 (2021).
- [13] G. M. Luke, Y. Fudamoto, K. M. Kojima, M. I. Larkin, J. Merrin, B. Nachumi, Y. J. Uemura, Y. Maeno, Z. Q. Mao, Y. Mori, H. Nakamura, and M. Sigrist, Time-reversal symmetry-breaking superconductivity in Sr_2RuO_4 , *Nature* **394**, 558 (1998).
- [14] G. Luke, Y. Fudamoto, K. Kojima, M. Larkin, B. Nachumi, Y. Uemura, J. Sonier, Y. Maeno, Z. Mao, Y. Mori, and D. Agterberg, Unconventional superconductivity in Sr_2RuO_4 , *Physica B: Condensed Matter* **289-290**, 373 (2000).
- [15] J. Xia, Y. Maeno, P. T. Beyersdorf, M. M. Fejer, and A. Kapitulnik, High Resolution Polar Kerr Effect Measurements of Sr_2RuO_4 : Evidence for Broken Time-Reversal Symmetry in the Superconducting State, *Phys. Rev. Lett.* **97**, 167002 (2006).
- [16] V. Grinenko, S. Ghosh, R. Sarkar, J.-C. Orain, A. Nikitin, M. Elender, D. Das, Z. Guguchia, F. Brückner, M. E. Barber, J. Park, N. Kikugawa, D. A. Sokolov, J. S. Bobowski, T. Miyoshi, Y. Maeno, A. P. Mackenzie, H. Luetkens, C. W. Hicks, and H.-H. Klauss, Split superconducting and time-reversal symmetry-breaking transitions, and magnetic order in Sr_2RuO_4 under uniaxial stress, *Nature Physics* **17**, 748.
- [17] K. Deguchi, Z. Q. Mao, and Y. Maeno, Determination of the Superconducting Gap Structure in All Bands of the Spin-Triplet Superconductor Sr_2RuO_4 , *Journal of the Physical Society of Japan* **73**, 1313 (2004).
- [18] E. Hassinger, P. Bourgeois-Hope, H. Taniguchi, S. René de Cotret, G. Grissonnanche, M. S. Anwar, Y. Maeno, N. Doiron-Leyraud, and L. Taillefer, Vertical Line Nodes in the Superconducting Gap Structure of Sr_2RuO_4 , *Phys. Rev. X* **7**, 011032 (2017).
- [19] R. Sharma, S. D. Edkins, Z. Wang, A. Kostin, C. Sow, Y. Maeno, A. P. Mackenzie, J. C. S. Davis, and V. Madhavan, Momentum-resolved superconducting energy gaps of Sr_2RuO_4 from quasiparticle interference imaging, *Proceedings of the National Academy of Sciences* **117**, 5222 (2020).
- [20] A. T. Rømer, D. D. Scherer, I. M. Eremin, P. J. Hirschfeld, and B. M. Andersen, Knight Shift and Leading Superconducting Instability from Spin Fluctuations in Sr_2RuO_4 , *Phys. Rev. Lett.* **123**, 247001 (2019).
- [21] H. G. Suh, H. Menke, P. M. R. Brydon, C. Timm, A. Ramires, and D. F. Agterberg, Stabilizing even-parity chiral superconductivity in Sr_2RuO_4 , *Phys. Rev. Research* **2**, 032023(R) (2020).
- [22] S. A. Kivelson, A. C. Yuan, B. Ramshaw, and R. Thomale, A proposal for reconciling diverse experiments on the superconducting state in Sr_2RuO_4 , *npj Quantum Materials* **5**, 43 (2020).
- [23] A. C. Yuan, E. Berg, and S. A. Kivelson, Strain-induced time reversal breaking and half quantum vortices near a putative superconducting tetracritical point in Sr_2RuO_4 , *Phys. Rev. B* **104**, 054518 (2021).
- [24] J. Clepkens, A. W. Lindquist, and H.-Y. Kee, Shadowed triplet pairings in Hund's metals with spin-orbit coupling, *Phys. Rev. Research* **3**, 013001 (2021).
- [25] J. Clepkens, A. W. Lindquist, X. Liu, and H.-Y. Kee, Higher angular momentum pairings in interorbital shadowed-triplet superconductors: Application to Sr_2RuO_4 , *Phys. Rev. B* **104**, 104512 (2021).
- [26] A. T. Rømer, P. J. Hirschfeld, and B. M. Andersen, Super-

- conducting state of Sr₂RuO₄ in the presence of longer-range Coulomb interactions, *Phys. Rev. B* **104**, 064507 (2021).
- [27] A. T. Rømer, T. A. Maier, A. Kreisel, P. J. Hirschfeld, and B. M. Andersen, Leading superconducting instabilities in three-dimensional models for Sr₂RuO₄, *Phys. Rev. Research* **4**, 033011 (2022).
- [28] X. Wang, Z. Wang, and C. Kallin, Higher angular momentum pairing states in Sr₂RuO₄ in the presence of longer-range interactions [10.48550/arXiv.2207.11180](https://arxiv.org/abs/10.48550/arXiv.2207.11180) (2022).
- [29] K. D. Nelson, Z. Mao, Y. Maeno, and Y. Liu, Odd-Parity Superconductivity in Sr₂RuO₄, *Science* **306**, 1151 (2004).
- [30] F. Kidwingira, J. D. Strand, D. J. V. Harlingen, and Y. Maeno, Dynamical Superconducting Order Parameter Domains in Sr₂RuO₄, *Science* **314**, 1267 (2006).
- [31] J. Jang, D. G. Ferguson, V. Vakaryuk, R. Budakian, S. B. Chung, P. M. Goldbart, and Y. Maeno, Observation of Half-Height Magnetization Steps in Sr₂RuO₄, *Science* **331**, 186 (2011).
- [32] X. Cai, B. M. Zakrzewski, Y. A. Ying, H.-Y. Kee, M. Sigrist, J. E. Ortman, W. Sun, Z. Mao, and Y. Liu, Magnetoresistance oscillation study of the spin counterflow half-quantum vortex in doubly connected mesoscopic superconducting cylinders of Sr₂RuO₄, *Phys. Rev. B* **105**, 224510 (2022).
- [33] Y. Asano, Y. Tanaka, M. Sigrist, and S. Kashiwaya, Josephson current in s-wave-superconductor/Sr₂RuO₄ junctions, *Phys. Rev. B* **67**, 184505 (2003).
- [34] K. Kawai, K. Yada, Y. Tanaka, Y. Asano, A. A. Golubov, and S. Kashiwaya, Josephson effect in a multiorbital model for Sr₂RuO₄, *Phys. Rev. B* **95**, 174518 (2017).
- [35] N. Hayashi, C. Iniotakis, M. Machida, and M. Sigrist, Josephson effect between conventional and Rashba superconductors, *Physica C: Superconductivity and its Applications* **468**, 844 (2008).
- [36] L. Klam, A. Epp, W. Chen, M. Sigrist, and D. Manske, Josephson effect and triplet-singlet ratio of noncentrosymmetric superconductors, *Phys. Rev. B* **89**, 174505 (2014).
- [37] I. Žutić and I. Mazin, Phase-Sensitive Tests of the Pairing State Symmetry in Sr₂RuO₄, *Phys. Rev. Lett.* **95**, 217004 (2005).
- [38] Y. A. Ying, N. E. Staley, Y. Xin, K. Sun, X. Cai, D. Fobes, T. J. Liu, Z. Q. Mao, and Y. Liu, Enhanced spin-triplet superconductivity near dislocations in sr2ruo4, *Nature Communications* **4**, 2596 (2013).
- [39] A. Umerski, Closed-form solutions to surface Green's functions, *Phys. Rev. B* **55**, 5266 (1997).
- [40] C. M. Puetter and H.-Y. Kee, Identifying spin-triplet pairing in spin-orbit coupled multi-band superconductors, *EPL (Europhysics Letters)* **98**, 27010 (2012).
- [41] S. Hoshino and P. Werner, Superconductivity from emerging magnetic moments, *Phys. Rev. Lett.* **115**, 247001 (2015).
- [42] S. Hoshino and P. Werner, Electronic orders in multiorbital hubbard models with lifted orbital degeneracy, *Phys. Rev. B* **93**, 155161 (2016).
- [43] A. Ramires and M. Sigrist, Identifying detrimental effects for multiorbital superconductivity: Application to Sr₂RuO₄, *Phys. Rev. B* **94**, 104501 (2016).
- [44] A. K. C. Cheung and D. F. Agterberg, Superconductivity in the presence of spin-orbit interactions stabilized by hund coupling, *Phys. Rev. B* **99**, 024516 (2019).
- [45] A. Ramires and M. Sigrist, Superconducting order parameter of Sr₂RuO₄: A microscopic perspective, *Phys. Rev. B* **100**, 104501 (2019).
- [46] W. Huang, Y. Zhou, and H. Yao, Exotic Cooper pairing in multiorbital models of Sr₂RuO₄, *Phys. Rev. B* **100**, 134506 (2019).
- [47] O. Gingras, R. Nourafkan, A.-M. S. Tremblay, and M. Côté, Superconducting Symmetries of Sr₂RuO₄ from First-Principles Electronic Structure, *Phys. Rev. Lett.* **123**, 217005 (2019).
- [48] S.-O. Kaba and D. Sénéchal, Group-theoretical classification of superconducting states of strontium ruthenate, *Phys. Rev. B* **100**, 214507 (2019).
- [49] A. W. Lindquist and H.-Y. Kee, Distinct reduction of Knight shift in superconducting state of Sr₂RuO₄ under uniaxial strain, *Phys. Rev. Research* **2**, 032055(R) (2020).
- [50] A. W. Lindquist, J. Clepkens, and H.-Y. Kee, Evolution of interorbital superconductor to intraorbital spin-density wave in layered ruthenates, *Phys. Rev. Research* **4**, 023109 (2022).
- [51] O. Gingras, N. Allaglo, R. Nourafkan, M. Côté, and A.-M. S. Tremblay, Superconductivity in correlated multiorbital systems with spin-orbit coupling: Coexistence of even- and odd-frequency pairing, and the case of Sr₂RuO₄, *Phys. Rev. B* **106**, 064513 (2022).

Appendix A: Tight-Binding Model

The form of the microscopic Hamiltonian is introduced in Sec. II. Here, we provide the dispersion terms used within that model, as well as the values used for various hopping parameters throughout this work. The dispersion of the *s*-wave and normal insulator regions are given by,

$$\begin{aligned}\xi_{A(B)}(\mathbf{k}, 0) &= -\mu_{A(B)} - 2t \cos k_x, \\ \xi_{A(B)}(\mathbf{k}, 1) &= t - 2t' \cos k_x.\end{aligned}\quad (\text{A1})$$

All hopping terms are limited to next nearest neighbor, such that the slab setup for the surface Green's functions features one layer of atoms at a time.

Next, the dispersion terms in the SRO region are given by,

$$\begin{aligned}\xi_C^{yz(xz)}(\mathbf{k}, 0) &= -\mu_{1D} - 2t_{2(1)} \cos k_x, \\ \xi_C^{xy}(\mathbf{k}, 0) &= -\mu_{xy} - 2t_3 \cos k_x, \\ \xi_C^{yz(xz)}(\mathbf{k}, \frac{1}{2}) &= 4t_z^{1D} \cos \frac{k_x}{2} \cos \frac{k_z}{2}, \\ \xi_C^{xy}(\mathbf{k}, \frac{1}{2}) &= 4t_z^{xy} \cos \frac{k_x}{2} \cos \frac{k_z}{2}, \\ \xi_C^{yz(xz)}(\mathbf{k}, 1) &= -t_{1(2)}, \\ \xi_C^{xy}(\mathbf{k}, 1) &= -t_3 - 2t_4 \cos k_x, \\ \xi_C^{yz/xz}(\mathbf{k}, \frac{1}{2}) &= 4t_6 i \sin \frac{k_x}{2} \cos \frac{k_z}{2}, \\ \xi_C^{yz/xy}(\mathbf{k}, \frac{1}{2}) &= -4t_7 \sin \frac{k_x}{2} \sin \frac{k_z}{2}, \\ \xi_C^{xz/xy}(\mathbf{k}, \frac{1}{2}) &= 4t_7 i \cos \frac{k_x}{2} \sin \frac{k_z}{2}, \\ \xi_C^{yz/xz}(\mathbf{k}, 1) &= 2t_{1D} i \sin k_x.\end{aligned}\quad (\text{A2})$$

Here, $\delta_y = \frac{1}{2}$ occurs with interlayer hopping in the *z*-direction due to the offset between layers. We also include

the A_{1g} , B_{2g} , and E_g SOC terms,

$$\begin{aligned}
H_{\text{SOC}} = & i\lambda \sum_{\mathbf{k}, i_y} \sum_{abl} \epsilon_{abl} c_{C, \mathbf{k}, i_y, \sigma}^{a\dagger} c_{C, \mathbf{k}, i_y, \sigma'}^b \hat{\sigma}_{\sigma\sigma'}^l \\
& + i \sum_{\mathbf{k}, i_y} \lambda^{B_{2g}}(k_x) \sigma_{\sigma\sigma'}^y (c_{C, \mathbf{k}, i_y, \sigma}^{xz\dagger} c_{C, \mathbf{k}, i_y+1, \sigma'}^{xy} \\
& \quad - c_{C, \mathbf{k}, i_y, \sigma}^{xz\dagger} c_{C, \mathbf{k}, i_y-1, \sigma'}^{xy}) \\
& - i \sum_{\mathbf{k}, i_y} \lambda^{B_{2g}}(k_x) \sigma_{\sigma\sigma'}^x (c_{C, \mathbf{k}, i_y, \sigma}^{yz\dagger} c_{C, \mathbf{k}, i_y+1, \sigma'}^{xy} \\
& \quad - c_{C, \mathbf{k}, i_y, \sigma}^{yz\dagger} c_{C, \mathbf{k}, i_y-1, \sigma'}^{xy}) \\
& + i \sum_{\mathbf{k}, i_y} \lambda^{E_g, x}(\mathbf{k}) \sigma_{\sigma\sigma'}^z (c_{C, \mathbf{k}, i_y, \sigma}^{xz\dagger} c_{C, \mathbf{k}, i_y+\frac{1}{2}, \sigma'}^{xy} \\
& \quad + c_{C, \mathbf{k}, i_y, \sigma}^{xz\dagger} c_{C, \mathbf{k}, i_y-\frac{1}{2}, \sigma'}^{xy}) \\
& - i \sum_{\mathbf{k}, i_y} \lambda^{E_g, y}(\mathbf{k}) \sigma_{\sigma\sigma'}^z (c_{C, \mathbf{k}, i_y, \sigma}^{yz\dagger} c_{C, \mathbf{k}, i_y+\frac{1}{2}, \sigma'}^{xy} \\
& \quad - c_{C, \mathbf{k}, i_y, \sigma}^{yz\dagger} c_{C, \mathbf{k}, i_y-\frac{1}{2}, \sigma'}^{xy}),
\end{aligned} \tag{A3}$$

where ϵ_{abl} is the completely antisymmetric tensor, the momentum dependent B_{2g} SOC, $\lambda^{B_{2g}}(k_x) = 2i\lambda_{B_{2g}} \sin k_x$, and the momentum dependent E_g SOCs, $\lambda^{E_g, x}(\mathbf{k}) = 4\lambda_{E_g} \sin \frac{k_x}{2} \sin \frac{k_z}{2}$ and $\lambda^{E_g, y}(\mathbf{k}) = 4i\lambda_{E_g} \cos \frac{k_x}{2} \sin \frac{k_z}{2}$. Finally, the hopping between regions B and C has the form,

$$\xi_{B/C}^a(k_x) = t_{B/C}^a - 2t'_{B/C} \cos k_x. \tag{A4}$$

t_1	t_2	t_3	t_4	t_5
0.51	0.06	0.5	0.18	0.02
t_6	t_7	t_z^{1D}	t_z^{xy}	μ_{1D}
-0.01	0.009	-0.025	0.002	0.52
μ_{xy}	λ	$\lambda_{B_{2g}}$	λ_{E_g}	t
0.63	0.1	-0.02	-0.0025	0.5
t'	μ_1	μ_2	$t_{B/C}^{yz}$	$t_{B/C}^{xz}$
0.2	0.18	-10	0.05	0.5
$t_{B/C}^{xy}$	$t_{B/C}^{yz}$	$t_{B/C}^{xz}$	$t_{B/C}^{xy}$	
0.5	0.02	0.2	0.2	

TABLE I. Tight-binding parameters used in all of the calculations presented in this work. The parameters for the SRO region were obtained from the DFT calculations presented in Ref. 25, but limited to nearest and next-nearest neighbor terms.

The SRO tight-binding parameters used in all of the calculations presented here were obtained from Ref. 25, and are listed in Table I. The SOC values used here are chosen to be similar to the values at which higher-angular momentum pairings were found to exist. The Fermi surface obtained using the listed tight-binding parameters is shown in Fig. 4 for the $k_z = 0$ plane.

The irreducible representation of each of the pairing states discussed in this work in terms of the interorbital parameters shown in Eq. (15) can be found in Ref. 25. In all calculations presented here we fix the magnitude of the $|\vec{\Delta}_{xz/xy}| = |\vec{\Delta}_{yz/xy}| = 1 \times 10^{-3}$ for consistency. In the s -wave case which also features finite $|\Delta_{yz/xz}^z|$, this value is set to 5×10^{-4} , all in units of $2t = 1$. Note that while the

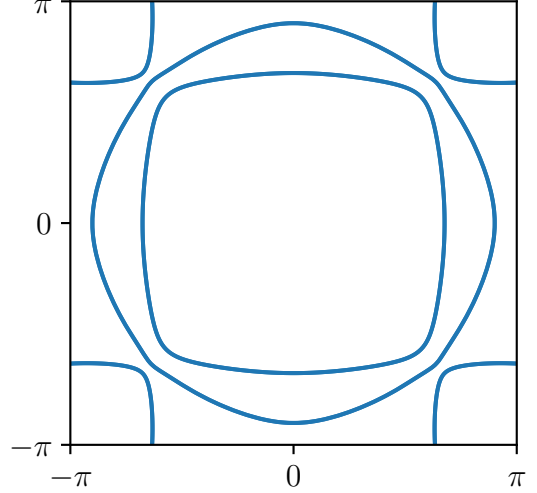


Figure 4. Fermi surface of SRO shown in the $k_z = 0$ plane, for the tight-binding parameters presented in Table I.

interorbital terms are chosen to be equal for all interorbital pairing states, this does not mean that the gap size is equal, as the gap size and nodal structure are determined by various parameters such as the SOC and dispersion terms.

Appendix B: Two Orbital Analysis

Insights into the mechanism by which the odd-parity behavior appears can be gained by considering a two-orbital model which can be solved analytically. The two-orbital Hamiltonian is presented in Eq. (16) shown in Section IV. Following the procedure presented in Ref. 25, this Hamiltonian is transformed into the band basis using,

$$\begin{bmatrix} c_{\mathbf{k}, \sigma}^a \\ c_{\mathbf{k}, \sigma}^b \end{bmatrix} = \begin{bmatrix} f_{\mathbf{k}\sigma} & -g_{\mathbf{k}\sigma} \\ g_{\mathbf{k}\sigma} & f_{\mathbf{k}\sigma} \end{bmatrix} \begin{bmatrix} c_{\mathbf{k}, \sigma}^\alpha \\ c_{\mathbf{k}, \sigma}^\beta \end{bmatrix}. \tag{B1}$$

The bands are denoted by α and β , index, and the transformation coefficients are,

$$\begin{aligned}
f_{\mathbf{k}\sigma} &= \frac{-t(\mathbf{k}) - i(\eta_\sigma \lambda(\mathbf{k})) - \alpha(\mathbf{k})}{\sqrt{t(\mathbf{k})^2 + (\eta_\sigma \lambda(\mathbf{k}) - \alpha(\mathbf{k}))^2}} \sqrt{\frac{1}{2} \left(1 + \frac{\xi^-(\mathbf{k})}{E'_\sigma(\mathbf{k})} \right)}, \\
g_{\mathbf{k}\sigma} &= -\sqrt{\frac{1}{2} \left(1 - \frac{\xi^-(\mathbf{k})}{E'_\sigma(\mathbf{k})} \right)}.
\end{aligned} \tag{B2}$$

Here, $\eta_\sigma = \pm 1$ for $\sigma = \uparrow, \downarrow$ and $E'_\sigma(\mathbf{k}) = \sqrt{\xi^-(\mathbf{k})^2 + 4(t(\mathbf{k})^2 + (\eta_\sigma \lambda(\mathbf{k}) - \alpha(\mathbf{k}))^2)}$ where the energy eigenvalues are $E_\sigma^\pm(\mathbf{k}) = \frac{1}{2}(\xi^+(\mathbf{k}) \pm E'_\sigma(\mathbf{k}))$.

In the orbital basis, the pairing Hamiltonian is written,

$$H_{\text{SC}} = \Delta_z (c_{-\mathbf{k}, \downarrow}^b c_{\mathbf{k}, \uparrow}^a - c_{-\mathbf{k}, \downarrow}^a c_{\mathbf{k}, \uparrow}^b + c_{-\mathbf{k}, \uparrow}^a c_{\mathbf{k}, \downarrow}^b - c_{-\mathbf{k}, \uparrow}^b c_{\mathbf{k}, \downarrow}^a). \tag{B3}$$

This is transformed into the band basis using the same transformation described above. Since we are only interested in the intraband pairing we neglect pairing terms between the α and β bands. The pairing in the band basis is

simplified using $f_{-\mathbf{k}\downarrow}^* = f_{\mathbf{k}\uparrow}$ and $g_{-\mathbf{k}\downarrow} = g_{\mathbf{k}\uparrow}$, and appears as,

$$H_{\text{pair}} = i\Delta_{a/b}^z \{ \text{Im}[g_{\mathbf{k}\uparrow}f_{\mathbf{k}\uparrow} + g_{-\mathbf{k}\uparrow}f_{-\mathbf{k}\uparrow}](\hat{\Delta}_0^\alpha(\mathbf{k}) - \hat{\Delta}_0^\beta(\mathbf{k})) \\ + \text{Im}[g_{\mathbf{k}\uparrow}f_{\mathbf{k}\uparrow} - g_{-\mathbf{k}\uparrow}f_{-\mathbf{k}\uparrow}](\hat{\Delta}_z^\alpha(\mathbf{k}) - \hat{\Delta}_z^\beta(\mathbf{k})) \}. \quad (\text{B4})$$

Since $f_{\mathbf{k}\sigma}$ and $g_{\mathbf{k}\sigma}$ are neither even nor odd in the presence of $\alpha(\mathbf{k})$, we perform a Taylor expansion of $\frac{1}{E'_\uparrow(\mathbf{k})}$ for small $\alpha(\mathbf{k})$.

$$\text{Im}[f_{\mathbf{k}\uparrow}g_{\mathbf{k}\uparrow}] = -\frac{\lambda(\mathbf{k}) - \alpha(\mathbf{k})}{2E'_\uparrow(\mathbf{k})} \\ = \frac{1}{2}(\lambda(\mathbf{k}) - \alpha(\mathbf{k})) \left\{ \frac{1}{\sqrt{\xi^-(\mathbf{k})^2 + 4(t(\mathbf{k})^2 + \lambda(\mathbf{k})^2)}} \quad (\text{B5}) \\ + \frac{4\lambda(\mathbf{k})\alpha(\mathbf{k})}{(\xi^-(\mathbf{k})^2 + 4(t(\mathbf{k})^2 + \lambda(\mathbf{k})^2))^{\frac{3}{2}}} + \mathcal{O}(\alpha(\mathbf{k})^2) \right\}.$$

Now, writing the even-parity pseudospin-singlet and odd-parity pseudospin-triplet terms are straightforward, and are shown in Eqs. (18) and (19), respectively. Eqs. (22) and (23) are obtained by instead assuming that the finite expectation value exists only in the intraorbital spin-singlet pairing channel. The same Taylor expansion is performed for the coefficients $|f_{\mathbf{k}\uparrow}|^2$ or $|g_{\mathbf{k}\uparrow}|^2$, however the lack of $\alpha(\mathbf{k})$ in the numerator of these terms leads to odd-parity contributions only arising from higher order terms.